Formation of arcs by nearly circular gravitational lenses

Roger D. Blandford
Institute of Astronomy, Cambridge, England
and Theoretical Astrophysics, California Institute of Technology, Pasadena, California 91125

Israel Kovner
Institute of Astronomy, Cambridge, England
and Physics Department, Weizmann Institute, Rehovot 76100, Israel
(Received 6 November 1987)

An extended source located near the axis of a nearly circular, sufficiently nonlinear lens can produce extended-arc-like images. Examples of these may have been found near three distant clusters of galaxies which seem to be acting as gravitational lenses. We propose a simple geometrical method for locating images of objects using the Einstein ring and the corresponding caustic. We also give an approximate theory of lenses for which deviations from circularity are small perturbations. We discuss noncircular perturbations of practical interest for gravitational lensing and properties of the arcs that are thus formed.

I. INTRODUCTION

Recently, almost circular "giant luminous arcs" associated with the cores of two distant clusters of galaxies (A370, 2242-02, and A963) were reported.[1] Gravitational lensing, one possible explanation for these arcs, has been proposed by several authors.[2] In this paper, we analyze the geometrical optics of an almost circular gravitational lens and elucidate the conditions under which extended arcs may be formed.

Although inspired by hypothetical gravitational-lens action, our analysis is quite general. As regards geometrical optics, lenses made of gravitational fields differ little from lenses made of other substances, such as glass for light or electromagnetic fields for electrons. Gravitational lenses are remarkable in that they are achromatic and because the cases so far discovered are at cosmological distances. The latter fact requires the use of non-Euclidean angular-diameter distances (the ratio of the transverse size of an object to its angular size) but this is not relevant for general features of the observed images.

Having in mind the astrophysical applications of gravitational lensing we restrict ourselves to these and assume achromaticity, geometrical optics, paraxiality (i.e., small angles of deflection), and a flat source (object). It is important to distinguish lenses used in common optical instruments from gravitational lenses. The former are usually constructed so that the deflection depends *linearly* on the positions of incoming and outgoing rays. This means that, typically, only one ray will connect points on opposite sides of a lens. Gravitational lenses are usually nonlinear in this sense; in particular, a point source may be connected to an observer by several rays. In fact, the expression *gravitational lens* is conventionally taken to imply the presence of multiple images of a more distant source, and it is by this means that the few examples we have were discovered (see recent reviews[3]).

We should also remember that in a gravitational lens there is generally only one point of relevance on the observer's side of the lens: our location in space. However, a telescope at this point can measure the directions of incoming rays. We are therefore interested in mapping the object plane onto the ray direction at the observer. It is conventional to use angular coordinates for an object point defined by the direction that the ray would have had at the observer had the lens been absent, and to introduce similar angular coordinates for the image. (See Fig. 1.) These angular coordinates lie in the source plane and image plane, respectively.

When the lens is circularly symmetric, we can define an optic axis passing through the observer position and the lens center. If the lens is strong enough, it will deflect rays from a small source on the optic axis towards the observer so that he will see a thin ring image centered on the optic axis. This is called the *Einstein ring*. If the source is displaced slightly off the optic axis, the observer will see an arc and a counter-arc lying near the Einstein ring and diametrically opposed with respect to the lens center.

The angular extent of each arc is the angular size of the source viewed from the axis: it is determined by the radial projections of the source on the Einstein ring. However, if a lens deviates slightly from circularity, this projection method is not applicable; it turns out that the arcs need not be diametrically opposed. In this paper, we present a simple approximate method for calculating the widths and lengths of the arc images.

In Sec. II we define notation and review the theory of thin lenses. This is specialized to the almost circular lens case in Sec. III, where the relations between the source and image positions with respect to critical curves and caustics are derived, and a simple construction that can be used to locate the image of a point source is described. A simple interpretation of this construction in three dimensions and a generalization to a thick lens are offered in Sec. IV.

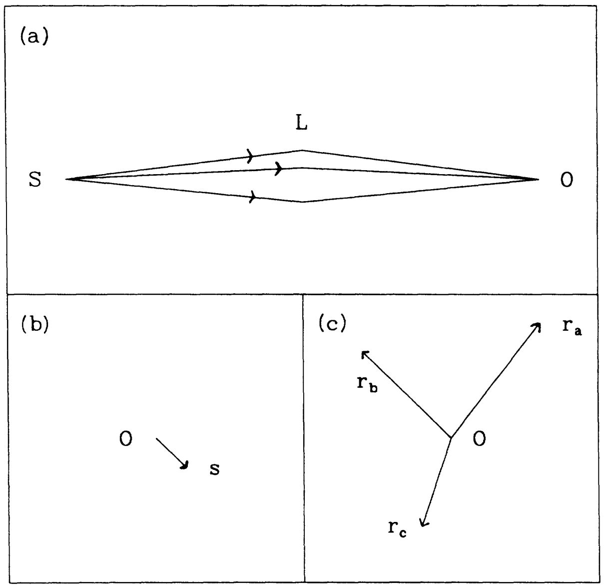

FIG. 1. Geometry of a nonlinear lens. (a) Rays leaving the source (S) are deflected by the lens (L) to meet at the observer (O). In this example, three images of a point source will be created. (b) Source plane, as seen by the observer. $\mathbf{s}$ is a small angle vector connecting the optic axis (O) to a point source. (c) Image plane as seen by the observer. $\mathbf{r}_a$, $\mathbf{r}_b$, and $\mathbf{r}_c$ are the positions of the three images.

II. THE THIN LENS

We make the paraxial (i.e., small-angle) approximation and measure the position of a point image on the sky, $\mathbf{r}=(x,y)$, by the projection of the unit vector in the direction to the image on a plane normal to a conveniently chosen lens axis. The axis corresponds to the origin in the approximately flat image plane. The position of the corresponding point source, $\mathbf{s}=(s_x,s_y)$, measured in the same way, is the position at which the source would be observed in the absence of the lens. A thin lens can be approximated by a deflection at a single thin screen. The lens equation, which relates the source position to the image position, is a Lagrangian mapping,

$$\mathbf{r}\to\mathbf{s}=\mathbf{r}-\nabla_{\mathbf{r}}\Phi(\mathbf{r}). \tag{2.1}$$

For a gravitational lens, the effective deflection $\nabla_{\mathbf{r}}\Phi$ is a gradient of a two-dimensional potential

$$\Phi=\frac{d_{\mathrm{LS}}}{d_{\mathrm{OL}}d_{\mathrm{OS}}}\int_{\text{line of sight}}\frac{2\phi_N}{c^2}dl, \tag{2.2}$$

where ϕ_N is the Newtonian gravitational potential and d_{OS}, d_{OL}, and d_{LS} are the observer-source, observer-lens, and the lens-source angular diameter distances, respectively (see Fig. 1). The quantity $(1-2\phi_N/c^2)$ behaves like a refractive index.[4] Φ satisfies Poisson's equation

$$\nabla^2\Phi=2\kappa(\mathbf{r}), \tag{2.3}$$

where

$$\kappa(\mathbf{r})=\sigma(\mathbf{r})/\sigma_{\mathrm{cr}}(z_l,z_s). \tag{2.4}$$

$\sigma(\mathbf{r})$ is the surface mass density of the lens, and the *critical density* σ_{cr} is determined by a combination of the angular diameter distances,

$$\sigma_{\mathrm{cr}}=\frac{c^2}{4\pi G}\frac{d_{\mathrm{OS}}}{d_{\mathrm{OL}}d_{\mathrm{LS}}}. \tag{2.5}$$

The shapes of images of sufficiently small sources can be described using either the *transformation* matrix

$$\mathcal{M}_{ij}=\frac{\partial s_i}{\partial r_j}=\delta_{ij}-\frac{\partial^2\Phi}{\partial r_i\partial r_j}, \tag{2.6}$$

or its inverse, $A_{ij}=M_{ij}^{-1}$, the *magnification* matrix which is symmetric for the thin lens.

Equation (2.1) must be solved to find images for a given source position. As the source is moved in the source plane $\{\mathbf{s}\}$, images can appear or disappear in pairs of opposite sign $\|\mathcal{M}\|$ (parity). If the mass distribution is bounded, transparent, and nonsingular, there is an odd number of images, and multiple imaging is possible if and only if $\|\mathcal{M}(\mathbf{r})\|<0$ somewhere in the sky[5] [the latter is guaranteed if $\kappa(\mathbf{r})>1$ somewhere.] We shall call the locus of merging solutions in the image plane *the critical lines,* and the corresponding lines in the source plane $\mathbf{s}$ *the caustic lines.* The inverse mapping, $\mathbf{s}\to\mathbf{r}$, is singular on caustics; in particular, the image magnification, $\|\mathcal{A}\|$, is divergent. Equivalently, at least one eigenvalue of $\mathcal{M}$ is zero and changes sign on crossing the critical line. The eigenvector of $\mathcal{M}$ with zero eigenvalue, the *degeneracy eigenvector* hereafter, gives the direction of infinite elongation of the images of an infinitesimal source located on the caustic. This direction is also the direction of a straight line connecting point images merging at this point on the critical line. The caustic lines are fold catastrophes which can exhibit singular points. The only generic singularity on a plane is a cusp, which occurs at points at which the degeneracy eigenvector is tangential to the critical line.[6] The degeneracy eigenvector as a function of a point on a critical curve is periodic for an even number of cusps and antiperiodic for an odd number of cusps.

Before applying perturbations, let us first consider a precisely circularly symmetric lens, with potential

$$\Phi(\mathbf{r})=f(r^2/2), \tag{2.7}$$

able to produce more than one image. This example is nongeneric. A source placed at the origin will, from Eq. (2.1), produce an Einstein ring image of radius r_o, satisfying

$$f'(r_o^2/2)=1. \tag{2.8}$$

(Note that the prime denotes differentiation with respect to the argument, $r^2/2$.) There can be more than one such ring (although this is astronomically unlikely), and if the potential is sufficiently regular at the center, there is also an image at the origin, $r=0$. The Einstein ring is in fact a critical line, the degeneracy eigenvector is tangential to the circle at its every point, and the corresponding caustic is a single point. We shall call these critical and caustic lines *tangential.* There may also be other critical curves. In particular, there may be a *radial* critical curve at which the radial eigenvalue of $\mathcal{M}$ vanishes. If a point source is displaced by a small distance from the center, there will be two diametrically opposed images near each Einstein ring, all the images, the source, and the origin lying on the same straight line (if there were a central image, it would remain close to the center).

In Sec. III we consider what happens in the generic case when the lens is not precisely circular. Also, we restrict ourselves to configurations producing arcs, i.e., we only study the results of perturbations on the tangential caustics and critical curves, while the radial ones concern us no further.

III. THE NEARLY CIRCULAR LENS

The tangential caustic associated with our exactly circular lens is a structurally unstable point and any small noncircular perturbation will cause it to unfold into a short continuous curve exhibiting at least four cusps (Fig. 2). Let the potential be written

$$\Phi(\mathbf{r})=f(r^2/2)+\epsilon\psi(r,\phi), \tag{3.1}$$

where the spherical part f is assumed to have only one tangential caustic; the perturbation parameter ϵ is small, $\epsilon \ll 1$; and the perturbing potential is arbitrary, except that the deflection which would be produced by the perturbation with $\epsilon=1$ is of the same order of magnitude as that produced by the spherical part of the potential $|\nabla f| \sim |\nabla\psi|$.

Let us consider an image point near the Einstein ring, $\mathbf{r}=(r_o+\Delta r)\mathbf{n}$, where the unit radial vector is

$$\mathbf{n}=(\cos\phi,\sin\phi), \tag{3.2}$$

and consider the position of a point source which would produce an image at this point,

$$\mathbf{s}=-\epsilon\nabla\psi(r_o,\phi)-\Delta r f''(r_o^2/2)r_o^2\mathbf{n}, \tag{3.3}$$

to first order in ϵ and in the displacement $\Delta\mathbf{r}=\mathbf{n}\Delta r$. Consider the positions of point sources which would produce images on a *guiding radius* $\phi=\phi_1=$ const near the critical circle. All these sources lie on a straight line or *spoke* parallel to $\mathbf{n}(\phi_1)$ and at a perpendicular distance

$$\Delta_\perp=\epsilon\mathbf{t}\cdot\nabla\psi\sim\epsilon r_o, \tag{3.4}$$

from the guiding radius, where

$$\mathbf{t}=(-\sin\phi\ ,\ \cos\phi) \tag{3.5}$$

is a unit tangential vector (Fig. 3).

For an approximately circular lens, this property can be used in reverse to locate the approximate image positions given a source position close to the origin. To do this, we must first locate the perturbed caustic and critical lines. The tangential critical lines are the loci of tangentially merging images (Fig. 4), so the tangential caustic is an envelope of the spokes. Since Δr is a curve parameter for a spoke given by Eq. (3.3), the envelope is given by the condition that the $\mathbf{t}$ component of the variation of Eq. (3.3) with respect to ϕ vanish:

$$-\epsilon\left[\frac{\partial\psi}{\partial r}+\frac{1}{r_o}\frac{\partial^2\psi}{\partial\phi^2}\right]_{\mathbf{r}=r_o\mathbf{n}}-r_o^2 f''(r_o^2/2)\Delta r_{\text{crit}}(\phi)=0, \tag{3.6}$$

where $\Delta r_{\text{crit}}(\phi)$ is the small radial perturbation of the critical curve. [Alternatively, we can require that the Jacobian of Eq. (2.1)

$$\|\mathcal{M}\|=\left[1-\frac{\partial^2\Phi}{\partial r^2}\right]\left[1-\frac{1}{r}\frac{\partial\Phi}{\partial r}-\frac{1}{r^2}\frac{\partial^2\Phi}{\partial\phi^2}\right]-\left[\frac{\partial}{\partial r}\frac{1}{r}\frac{\partial\Phi}{\partial\phi}\right]^2=0, \tag{3.7}$$

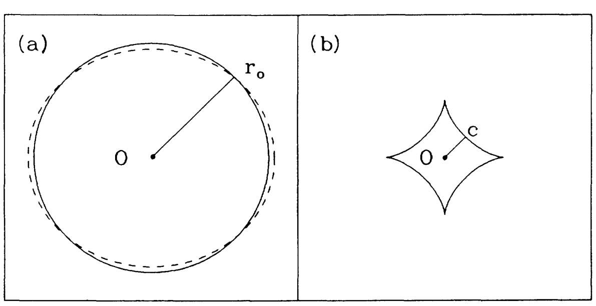

FIG. 2. Influence of noncircular perturbations. (a) Image plane. A circular lens will produce a critical circle (solid line) radius r_o. When a noncircular perturbation is applied, in this case proportional to $\cos 2\phi$, the critical circle is deformed into an ellipse (dashed line). (b) Source plane. The perturbation modifies the caustic from a degenerate point at O to a curve $\mathbf{c}(\phi)$, in this case a four-cusped asteroid.

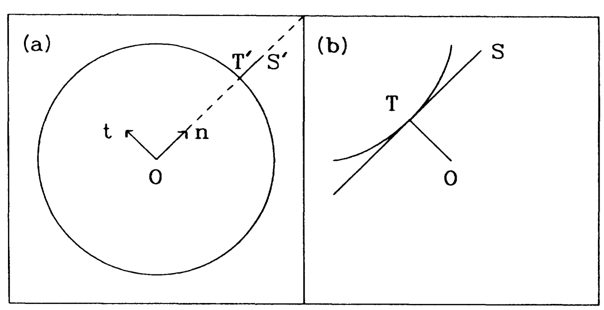

FIG. 3. Mapping from the image plane to the source plane with an almost circular lens. (a) Critical circle in the image plane. (b) The source plane in the vicinity of the caustic. [This diagram is magnified with respect to (a)]. A tangent is shown touching the caustic curve at T. Sources lying on the line segment TS will produce images lying on the segment $T'S'$ in the image plane. The lines TS and $T'S'$ are parallel to $\mathbf{n}$ and orthogonal to $\mathbf{t}$.

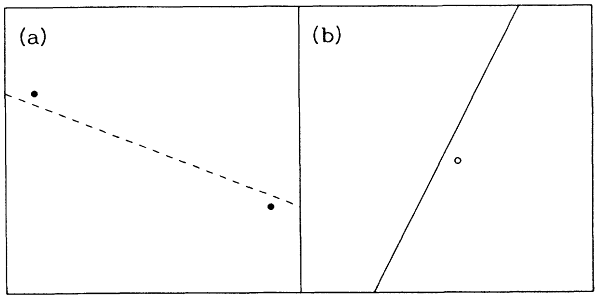

FIG. 4. Behavior of images near a critical line. (a) In a tangential merger, the image separation vector (degeneracy eigenvector) lies almost parallel to the critical line (dashed line). (b) The source (open circle) lies close to the caustic (solid line) which is orthogonal to the degeneracy eigenvector connecting the two image points in (a) (when the lens is thin).

vanish on the perturbed critical curve to derive Eq. (3.6).] Mapping this perturbation to the source plane using Eq. (3.3) gives the equation for the caustic curve:

$$\mathbf{c}(\phi)=\frac{\epsilon}{r_o}\left[\mathbf{n}\frac{\partial^2\psi}{\partial\phi^2}-\mathbf{t}\frac{\partial\psi}{\partial\phi}\right]_{\mathbf{r}=r_o\mathbf{n}}+O(\epsilon^2). \tag{3.8}$$

Note that the caustic depends only on the tangential derivatives of ψ at the Einstein ring to first order in ϵ, and that the curve parameter ϕ is the polar angle of the relevant point on the critical curve, not to be confused with the polar angle of the point on the caustic.

We are now in a position to describe a geometrical construction for locating the images of a point source near the center of a nearly circular lens with known potential (see Fig. 5).

(i) Draw the caustic $\mathbf{c}(\phi)$ given by Eq. (3.8), allowing ϕ to increase from 0 to 2π.

(ii) Draw the Einstein circle with radius r_o given by Eq. (2.8).

(iii) Draw all tangents from the source (S) to the caustic (points of tangency T_i) and extend them parallel to the guiding radius $\phi=\phi_i$ until they intersect the ring PTO.

The sense of the direction of extension of the tangent, given formally by Eq. (3.8), can usually be determined by inspection. In particular, if we know that the lens is overfocusing (i.e., producing a larger than average deflection) along some direction $\mathbf{n}$, then the relevant tangent point must be on the opposite side of the caustic from the image. If we determine the sense of extension for one direction, then the senses for all other directions can be obtained by continuously sliding the tangent along the caustic curve.

The intersections of the tangents with the ring give image positions with error $|\Delta\mathbf{r}_i|\sim\epsilon r_o\sim s\sim$ the size of the caustic. We illustrate this construction with some examples in Sec. V. A reduction in the tangential error would require a higher order approximation of the lens equation, since the direction of a tangent (a spoke) deviates from the direction of the corresponding $\mathbf{n}$ (a guiding radius) by $O(\epsilon)$. The radial error can be improved to $O(\epsilon^2 r_o)$ within Eq. (3.3), by the following additional construction.

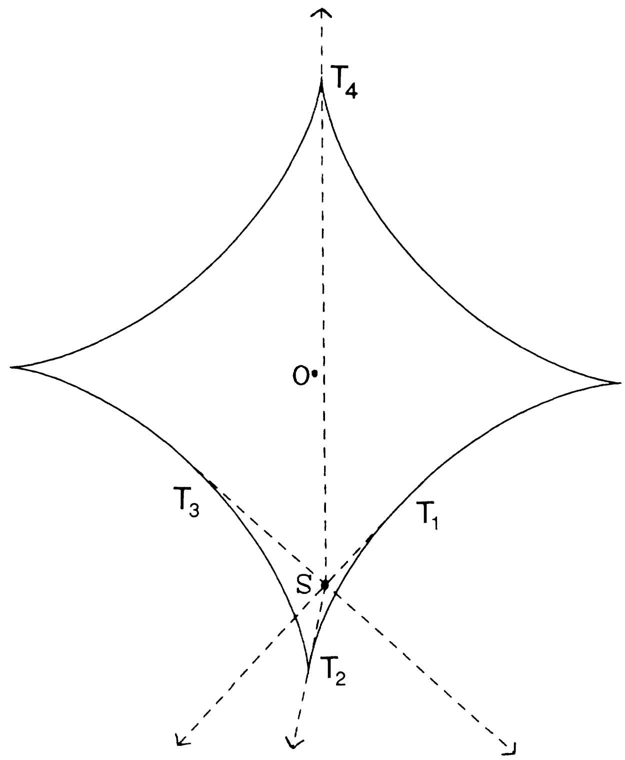

FIG. 5. Illustration of geometrical construction for locating the images of a point source S located near the caustic. In this case, the four images are formed along directions parallel to tangents of the caustic passing through S. The points of tangency are designated T_1, T_2, T_3, T_4. A source lying within the caustic therefore produces four images near the critical curve. A source just outside the caustic has two tangents which produce two images.

(a) Draw the perturbed critical line given by $r(\phi)=r_o+\Delta r_{\text{crit}}(\phi)$, where r_o and Δr_{crit} are determined by Eqs. (2.8) and (3.6), respectively.

(b) Measure the distance T_iS and place an image on the tangent at a radial distance $-T_iS/f''(r_o^2/2)r_o^2$ from the perturbed critical line.

For sources for which our construction is applicable, the tangents to caustics often pass near a cusp. This implies a further simplification: image positions can be roughly approximated by points of intersection of the Einstein ring with straight lines connecting the source and the cusps. For a point source inside and near a cusp, three nearby images are formed.

The positions and the number of the cusps can be found in the following way. Cusps are points at which the direction of a tangent to the caustic is reversed. The direction of the tangent $\mathbf{c}(\phi)$ is given by

$$\frac{d\mathbf{c}}{d\phi}=D(\phi)\mathbf{n}+O(\epsilon^2), \tag{3.9}$$

where

$$D(\phi)=\frac{\epsilon}{r_o}\left[\frac{\partial^3\psi}{\partial\phi^3}+\frac{\partial\psi}{\partial\phi}\right]_{\mathbf{r}=r_o\mathbf{n}}. \tag{3.10}$$

At a cusp, $D(\phi)=0$ and changes sign.

If the perturbation is sufficiently regular that the tangential critical curve and $D(\phi)$ are continuous, then $D(\phi)$ must be periodic with period 2π. This is because the curve is nearly circular and the degeneracy eigenvector is nearly tangent along all of it, so it must turn by 2π when traced along the curve. Therefore, the number of zeros and hence the number of cusps must be even. We now prove that the number of cusps is at least 4 for a continuous $D(\phi)$. Consider the expansion of $D(\phi)$ in a Fourier series. From the definition, Eq. (3.10), the Fourier coefficients of the constant and the fundamental terms are zero. In other words, the average,

$$\int_0^{2\pi} D(\phi)d\phi=0, \tag{3.11}$$

vanishes, and the convolution,

$$\int_0^{2\pi} D(\phi)\cos(\phi-\phi_0)d\phi=0 \tag{3.12}$$

vanishes for any phase ϕ_0. Any continuous periodic function of zero average must have at least two zeros within a period. Let ϕ_1,ϕ_2 be two zeros separated by $|\phi_1-\phi_2|\le\pi$ and suppose that these were the only two zeros. Now let $\phi_0=(\phi_1+\phi_2)/2$. It is then straightforward to see that the integral (3.12) cannot be zero. At least *four* zeros are required, and so at least four cusps must be produced in a perturbed tangential caustic.

It must be emphasized that this result only applies to tangentially merging images created by a perturbed circular lens easily able to produce multiple images. Two cusped caustics can be produced by nearly circular marginal[7] lenses. However, these cannot be treated by a perturbation approach.

IV. GEOMETRICAL INTERPRETATION

The constructions of the previous sections based on the two-dimensional (2D) mappings have a simple interpretation in terms of traditional[8] three-dimensional ray tracing. We consider a lens with its axis directed to the point on the sky taken to be the origin of our 2D coordinates, and we trace the light rays backwards in time: the rays emanate from the observer. The "image plane" is the set of directions of the rays at the observer. All the source points are assumed to lie in a "physical" source plane normal to the lens axis, the projection of this plane on the sky is what we call a "source plane." By a conjugate point we shall understand any point on a ray at which the number of other rays connecting it to the observer changes as we move along the ray[9] (rather than only the traditional[8] first such point). The conjugate points lie in caustic surfaces which are also envelopes of the rays.

There may be several caustic surfaces, but we consider only one which envelops the rays which merge approximately tangentially, in a nearly circular lens. Its section at the physical source plane projected on the sky is the tangential caustic introduced in Sec. III, the rays connecting this section to the observer form the critical line in the image plane. Consider one of the critical line rays and a thin pencil of adjacent rays. The cross section of this pencil (by a plane normal to the axis) is roughly circular near the observer but becomes very narrow near the physical source plane. The cross section of an infinitesimally thin pencil becomes linear (Fig. 6), tangential to the caustic at the conjugate point. This line is a *spoke*. Now let us displace the pencil slightly. A tangential displacement shifts the cross section to another conjugate point; a radial displacement shifts the cross section along itself, so it remains on the same spoke: the guiding radius in the vicinity of the critical line is mapped onto the parallel spoke in the vicinity of the tangential caustic.

Let us now consider the relative orientation of a spoke and its guiding radius, starting from a perfectly circular lens. In a thin circular lens, any ray lies in an axial plane, a tangential caustic surface degenerates to a line segment on the axis, all spokes are radial and collinear with their guiding radii. A small nonradial perturbation deflects the spokes sideways, so they remain approximately collinear with their guiding radii up to an error of order $O(\epsilon)$ in their direction. This explains our approximate method for a thin lens.

The same method with a small modification can also be applied to an almost circular thick lens, in which there are two or more separate lenses along the line of sight. In this case, there can be more than one Einstein ring and consequently more than one arc.

The method can also be adapted for use with almost circular electron lenses. In this case, the unperturbed deflection angle need not be derivable from a scalar potential and will have a curl. It turns out that the effect of this is simply to shift the source position, and arclike features could also be observed.

V. EXAMPLES OF PERTURBATIONS

The illustrations below are provided by first few harmonics of the multipole expansion

$$\psi(\mathbf{r})=\sum_n \psi_n(r)\cos n(\phi-\alpha_n). \tag{5.1}$$

Since image locations are determined by the angular dependence of ψ at the Einstein ring, we substitute r_o for

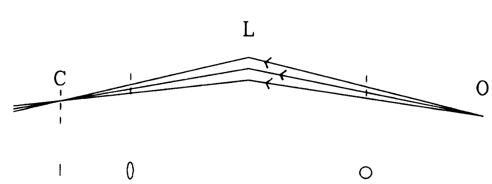

FIG. 6. Evolution of ray congruence in three dimensions. A thin pencil of rays travelling backwards from the observer O will be converged and sheared by the lens L. A pencil with circular cross section close to O will develop an elliptical cross section behind the lens which will degenerate to a line (spoke) at the conjugate point C. The rays and the spoke are both tangent to the caustic surface at the conjugate point.

r. There are types of lens models for which this expansion is useful. For instance, if the angular scale of variation of the perturbation over the sky is very much greater than r_o, a Taylor expansion of the potential is appropriate. Its first-order terms (a dipole) are a first harmonic, the second order contains a monopole and a quadrupole, the third order contains a dipole and a third harmonic, etc. An example of a great usefulness for modeling is an elliptic potential, dominated by its monopole and quadrupole moments. A practical model for lensing by clusters of galaxies is that of a group of several circular potential wells

$$\Phi(\mathbf{r})=\sum_{l=1}^{n} f_l[(\mathbf{r}-\mathbf{d}_l)^2/2], \tag{5.2}$$

where the origin is taken at a convenient point, e.g., the center of the dominant component or the center of mass, etc. If the separations between the centers $\sim d$ are smaller, then the *common* Einstein radius, r_o, defined by

$$\sum_l f_l(r_o^2/2)=1, \tag{5.3}$$

the potential can be approximated by a Taylor expansion in powers of the coordinates of the centers of the components (again, the first-order terms are a dipole moment, the second-order terms contain a quadrupole, etc.). Only the structure of the potential at the "common" Einstein ring is important: the perturbation can be very structured far inside the ring and still be dominated by low harmonics in its effect on the tangential caustic.

Let us now investigate examples of low harmonics. The first harmonic, $\psi_1(r)\cos(\phi-\alpha_1)$, as it follows from Eq. (3.7), only shifts the caustic point to

$$\mathbf{c}=\epsilon[\psi_1(r_o)/r_o](\sin\alpha_1,-\cos\alpha_1). \tag{5.4}$$

The action is simply that of a prism deflecting all the rays through a constant angle.

The second harmonic, a quadrupole, is the simplest nontrivial case. The source plane caustic is a four-cusped asteroid given by the parametric equation

$$\begin{aligned} c_x&=(-4\epsilon\psi_2/r_o)\cos^3\phi,\\ c_y&=(4\epsilon\psi_2/r_o)\sin^3\phi, \end{aligned} \tag{5.5}$$

setting $\alpha_2=0$ without loss of generality [Fig. 7(a)]. Four tangents pass through a source point lying within the asteroid, and therefore four images are produced at the critical circle. When the source point lies outside the caustic only two images are created.

The third harmonic produces a degenerate caustic, as does any odd-order harmonic,

$$\begin{aligned} c_x&=-(3\epsilon\psi_3/r_o)(2\cos2\phi+\cos4\phi),\\ c_y&=(3\epsilon\psi_3/r_o)(2\sin2\phi-\sin4\phi) \end{aligned} \tag{5.6}$$

(for $\alpha_3=0$) [Fig. 7(b)]. This is the parametric equation for a three-cusped deltoid, which is traced twice as $\mathbf{n}$ rotates through 2π so that the actual number of cusps is 6. A small perturbation will remove the degeneracy and bring out all the six cusps. Note that because the caustic is traced twice, the number of images changes by ±4 when the source crosses the deltoid.

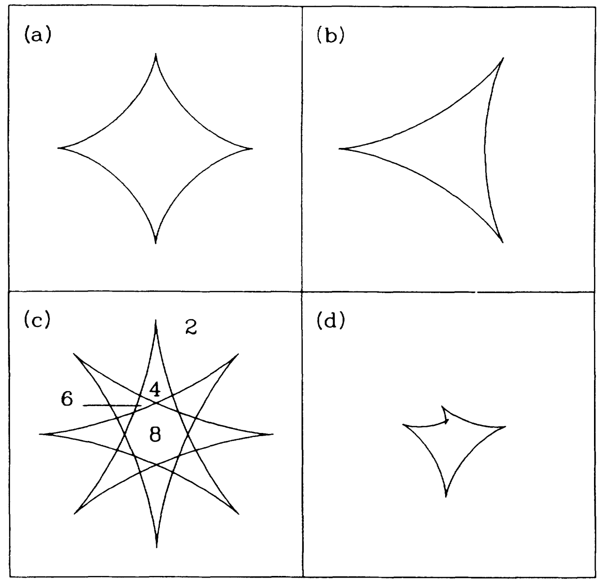

FIG. 7. Simple types of caustic produced by a nearly circular lens. (a) Four-cusped asteroid produced by a nonradial perturbation $\psi_2\cos2\phi$. (b) Three-cusped deltoid produced by a perturbation $\psi_3\cos3\phi$. This case is in fact degenerate and the curve is traced twice as ϕ advances from 0 to 2π. An additional perturbation will produce a six-cusped figure. Six images are created by a source located within the caustic and two by a source outside the caustic. (c) Eight-cusped octoid produced by a perturbation proportional to $\cos4\phi$. The number of images associated with each region of the diagram is indicated. (d) Mixture of $\cos2\phi$ and $\cos3\phi$ perturbations showing the change from four to six cusps through a swallowtail catastrophe.

The fourth harmonic produces a self-intersecting caustic,

$$\begin{aligned} c_x&=16\epsilon\psi_4/r_o(5\cos^3\phi-6\cos^5\phi),\\ c_y&=16\epsilon\psi_4/r_o(5\cos^3\phi-6\cos^5\phi). \end{aligned} \tag{5.7}$$

There are eight cusps [Fig. 7(c)]. A source lying completely outside the caustic produces two images near the Einstein ring. As it is moved towards the origin, the number of images changes by 2 each time a caustic line is crossed, giving a total of eight images when the source is near the origin.

It is interesting to see transitions between various types of caustics. An example of such is the combination of second and third harmonics,

$$\psi(\mathbf{r})=\psi_2(\mathbf{r})\cos2\phi+\psi_3(\mathbf{r})\cos3(\phi-\alpha_3), \tag{5.8}$$

which demonstrates the transition between four-cusp and six-cusp caustics. The boundary in the function space between the four-cusp and the six-cusp caustics is itself a curve of the same type as the source plane caustics. This can be seen by defining the perturbation ψ by two constants,

$$a \equiv \frac{\psi_3(r_o)}{\psi_2(r_o)}, \tag{5.9}$$

and α_3. Now let this 2D parameter space be a plane $\{\mathbf{a}\}$ with polar coordinates (a,α_3). Then the boundary in this parameter space between four-cusp and six-cusp caustics can be computed by noting that the number of cusps equals the number of roots of the equation $D(\Phi)=0$, where $D(\Phi)$ is given by Eq. (3.10). The result is an asteroidlike curve, given in a parametric form by

$$\mathbf{a}(\chi)=\left[\cos^3\chi\left[1-\tfrac{2}{3}\cos 2\chi\right],\sin^3\chi\left[1+\tfrac{2}{3}\cos 2\chi\right]\right], \quad 0\le\chi<2\pi . \tag{5.10}$$

As we change the potential so as to cross the curve, there will be a transition between the four-cusp and six-cusp caustics via a swallowtail singularity [Fig. 7(d)].

VI. FORMATION OF ARCS BY EXTENDED SOURCES

Point sources create point images. However, extended sources create arclike images. We can use the construction in its simpler and less accurate version to determine the approximate arc lengths by drawing the common tangents to the source and the caustic (see Fig. 8). The intersection of these limiting spokes with the critical circle will mark the ends of the arcs. The thickness of the arc will be proportional to the length of spoke crossing the source. A large source (of size $s > \sim\epsilon r_o$) that covers the caustic will create a complete circular image of radius r_o and thickness $\sim s$. A small source (of size $s \ll \epsilon r_o$) will usually only produce short arcs. However, when the source is located close to a cusp an extended arc can be produced. For an asteroid caustic created by a quadrupole perturbation, each source point within the caustic will map onto three image points on an extended arc and one image point on a shorter counterarc. If the source does not cover the caustic, then discontinuous arc segments will be created. The merging of these discontinuous segments is governed by the caustic-touching theorem.[10] Some more examples of continuous and discontinuous arcs are shown in Fig. 9.

It is important to realize that the length of the counterarc can be very short compared with the length of the main arc. If we take the simplest example of an asteroid caustic and assume that we have a circular source which lies within and just touches two branches of the caustic curve, then the arc lengths will be functions of the ratio of the radius of the source to the arm length of the asteroid caustic. For example, when this ratio is 0.1, the arc is 113° long and yet the counterarc is only 7° long. In a more contrived example, a line source extending from the origin to the cusp will produce a 180° arc and an infinitesimal counterarc.

Although our discussion so far has been couched in the framework of nearly circular lenses, it is possible to relax this requirement. It can happen that the critical line of a noncircular lens contains a nearly circular segment which is mapped onto a cusp or several cusps in the source plane. If a small source is located close to this part of the caustic, then the geometrical construction described in Sec. IV is valid for the images near the round part of the critical curve, with a possible correction for the dipole

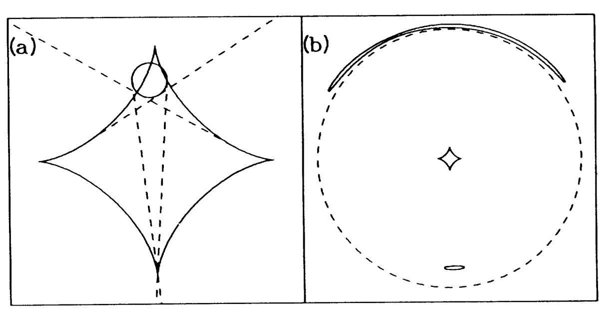

FIG. 8. Arc formation by an extended source. (a) In this example, a circular source is located close to a cusp. (b) An arc and a shorter counterarc are formed. The limits of these arcs can be located by drawing the common tangents (spokes) to the caustic and the source in the source plane. The arcs are bounded by the intersection of these tangents with the critical circle. The arc thickness is proportional to the length of the chord formed when a spoke crosses the source.

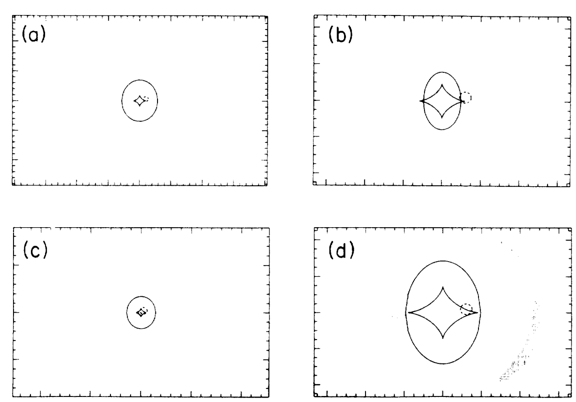

FIG. 9. Images of circular sources computed for noncircular lenses of different ellipticities. The solid lines are caustics, the dashed circle delineates the source. When the ellipticity of the lens is small the arcs are located close to the position given by the approximate constructions. However, the method is less precise for lenses of larger ellipticity. (a) A long arc and a small counterarc, small ellipticity. (b) A large arc and a tiny counterarc, large ellipticity. (c) An almost complete Einstein circle, small ellipticity. (d) A discontinuous arc, large ellipticity.

moment (a translation of the caustic with respect to the lens on the sky). The departure from circular symmetry need not be weak in this case. However, a counterarc would not necessarily lie on the same circle as the main arc or even exist. If the giant luminous arcs are indeed produced by gravitational lensing of distant galaxies, the absence of the counterarcs may also be due to a configuration of this kind. The fractional accuracy of our construction in this case is given by the ratio of the size of the relevant part of the caustic to the radius of the relevant part of the critical curve.

VII. CONCLUSION

In this paper we have derived a simple geometrical construction for locating images formed by a nearly circular lens in the vicinity of a nearly circular critical curve, for a point source in the vicinity of the corresponding caustic curve. This construction leads to understanding how a small extended source can be imaged as a single extended arc or several such arcs. We find that a similar construction is applicable for a thick lens. We hope that this construction may be helpful in understanding the structure of the gravitational fields of clusters A370, A963, and 2242-02, if the giant luminous arcs are indeed gravitationally lensed images of distant galaxies.

ACKNOWLEDGMENTS

We thank the Institute of Astronomy, Cambridge, where the first stages of this work were carried out, for hospitality. We also thank M. V. Berry, I. Frishman, and R. Nityananda for helpful discussions. R.B. acknowledges support under National Science Foundation Grant No. AST 86-15325. I.K. acknowledges support under SERC Grant No. SG/C 22555.

[1]G. Soucail, B. Fort, Y. Mellier, and J. P. Picat, Astron. Astrophys. **172**, L14 (1987); R. Lynds and V. Petrosian, Bull. Am. Astr. Soc. **18**, 1014 (1986); Astrophys. J. (to be published); R. J. Lavery and J. P. Henry, *ibid.* (to be published).

[2]B. Paczyński, Nature **325**, 572 (1987); I. Kovner, *ibid.* **327**, 193 (1987); G. Soucail, Y. Mellier, B. Fort, F. Hammer, and G. Mathez, Astron. Astrophys. (Lett.) **184**, L7 (1987); G. Soucail, Y. Mellier, B. Fort, G. Mathez, and M. Cailloux, *ibid.* **191**, L19 (1988); I. Kovner, in *The Post-Recombination Universe, NATO Advanced Study Institute, Series B: Physics,* edited by N. Kaiser and A. N. Lasenby (Reidel, Dordrecht, in press); S. Refsdal, *ibid.*; S. Grossman, and R. Narayan, Astrophys. J. (Lett.) **324**, L37 (1988); D. Narasimha and S. M. Chitre (to be published).

[3]C. R. Canizares, in *International Astronomical Union Symposium 124, Observational Cosmology*, edited by A. Hewitt, G. Burbidge, and L.-G. Fang (Reidel, Dordrecht, 1987), p. 729; R. D. Blandford and C. S. Kochanek, in *13th Jerusalem Winter School on Dark Matter in the Universe*, edited by T. Piran, J. Bahcall, and S. Weinberg (World Scientific, Singapore, 1987).

[4]C. W. Misner, K. S. Thorne, and J. A. Wheeler, *Gravitation* (Freeman, San Francisco, 1973).

[5]W. L. Burke, Astrophys. J. (Lett.) **244**, L1 (1981).

[6]V. L. Arnold, *Catastrophe Theory* (Springer-Verlag, Berlin, 1984); M. V. Berry and C. Upstill, Prog. Opt. **18**, 257 (1980).

[7]R. D. Blandford and R. Narayan, Astrophys. J. **310**, 568 (1987); I. Kovner, *ibid.* **321**, 686 (1987).

[8]M. Born and E. Wolf, *Principles of Optics*, 3rd ed. (Pergamon, Oxford, 1959).

[9]S. W. Hawking and G. F. R. Ellis, *The Large Scale Structure of Spacetime* (Cambridge University Press, Cambridge, England, 1973).

[10]M. V. Berry, J. Opt. Soc. Am. A. **4**, 561 (1987).

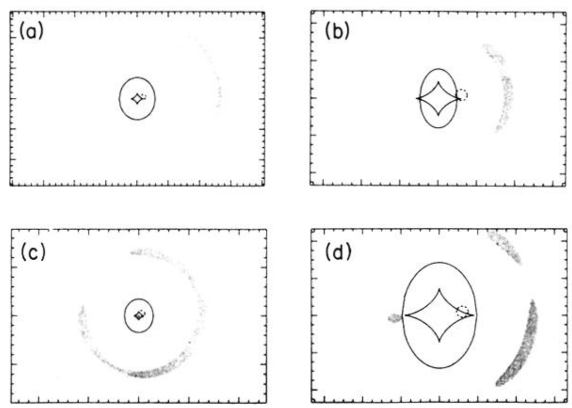

FIG. 9. Images of circular sources computed for noncircular lenses of different ellipticities. The solid lines are caustics, the dashed circle delineates the source. When the ellipticity of the lens is small the arcs are located close to the position given by the approximate constructions. However, the method is less precise for lenses of larger ellipticity. (a) A long arc and a small counterarc, small ellipticity. (b) A large arc and a tiny counterarc, large ellipticity. (c) An almost complete Einstein circle, small ellipticity. (d) A discontinuous arc, large ellipticity.